

A Single Crystal Study of $RE_{14}Co_3In_3$ ($RE = Y, Tb, Dy, Ho, Er$)

Vasyl' I. Zaremba^a, Yaroslav M. Kalychak^a, Mariya V. Dzevenko^a, Ute Ch. Rodewald^b, Birgit Heying^b, and Rainer Pöttgen^b

^a Inorganic Chemistry Department, Ivan Franko National University of Lviv, Kyryla and Mephodiya Street 6, 79005 Lviv, Ukraine

^b Institut für Anorganische und Analytische Chemie, Westfälische Wilhelms-Universität Münster, Corrensstraße 30, D-48149 Münster, Germany

Reprint requests to R. Pöttgen. E-mail: pottgen@uni-muenster.de

Z. Naturforsch. **61b**, 23–28 (2006); received December 13, 2005

The rare earth–cobalt–indides $RE_{14}Co_3In_3$ ($RE = Y, Tb, Dy, Ho, Er$) were prepared in polycrystalline form from the elements by arc-melting. Small single crystals were grown through a special annealing sequence. The compounds were investigated on the basis of X-ray powder and single crystal data: $Lu_{14}Co_2In_3$ ($Gd_{14}Co_3In_{2.7}$) type, $P4_2/nmc$, $Z = 4$, $a = 959.0(1)$, $c = 2319.1(5)$ pm, $wR2 = 0.055$, 2289 F^2 values, 65 variables for $Y_{13.90}Co_{2.99}In_{3.02}$, $a = 953.8(1)$, $c = 2315.8(5)$ pm, $wR2 = 0.108$, 2357 F^2 values, 65 variables for $Tb_{13.92}Co_{3.01}In_{2.92}$, $a = 949.24(3)$, $c = 2296.5(1)$ pm, $wR2 = 0.129$, 2518 F^2 values, 65 variables for $Dy_{13.90}Co_{2.97}In_{2.95}$, $a = 946.3(1)$, $c = 2289.0(5)$ pm, $wR2 = 0.099$, 2297 F^2 values, 64 variables for $Ho_{14}Co_{2.80}In_{2.89}$, and $a = 941.0(1)$, $c = 2274.2(5)$ pm, $wR2 = 0.140$, 2450 F^2 values, 65 variables for $Er_{13.83}Co_{2.88}In_{3.10}$. All $RE_{14}Co_3In_3$ indides show a small degree of In/Co mixing (between 7 and 16% Co) on the 4c In1 site and defects on the 8g Co1 positions (between 84 and 95% Co). Except for the holmium compound, the $RE_{14}Co_3In_3$ intermetallics also reveal RE/In mixing on the 4c RE1 sites, leading to the refined compositions. The seven crystallographically independent RE sites have between 9 and 10 nearest RE neighbors. The $RE_{14}Co_3In_3$ structures consist of a complex intergrowth of rare earth based polyhedra. Both cobalt sites have a distorted trigonal-prismatic rare earth coordination. An interesting feature is the In2–In2 dumb-bell with an In2–In2 distance of 300 pm (for $Ho_{14}Co_{2.80}In_{2.89}$). The crystal chemistry of the $RE_{14}Co_3In_3$ indides is discussed.

Key words: Rare Earth Compounds, Intermetallics, Crystal Chemistry

Introduction

The structural chemistry of rare earth (RE)–transition metal (T)–indides with a high RE content is characterized by high coordination numbers and chemical bonding is governed significantly by the many RE–RE contacts. The structures can be described by a complex packing pattern of different polyhedra [1, 2]. An overview is given in a recent review [3]. Although the RE–T–In systems are rich in compounds, so far only few RE-rich phases have been reported, *i. e.* $RE_{12}Ni_6In$ ($RE = Y, La, Pr, Nd, Sm, Gd$) and $RE_{12}Co_6In$ ($RE = La, Pr, Nd, Sm$) with $Sm_{12}Ni_6In$ type [1, 2, 4], RE_6Co_2In ($RE = Y, Sm, Gd–Ho, Tm, Lu$) with Ho_6Co_2Ga structure [2, 5], $RE_{14}Co_2In_3$ ($RE = Y, Gd–Tm, Lu$) [6] with $Lu_{14}Co_2In_3$ type, Er_5Ni_2In and $Tm_{4.83(3)}Ni_2In_{1.17(3)}$ [7] with Mo_5SiB_2 structure, and the series $RE_{12}Pt_7In$ ($RE = Ce, Pr, Nd, Gd, Ho$) [8] with an ordered version of the Gd_3Ga_2 type.

A discrepancy occurred for the gadolinium-based indide $Gd_{14}Co_3In_{2.7}$ [9] and the series $RE_{14}Co_2In_3$ ($RE = Y, Gd–Tm, Lu$) [6] where the structure was originally determined from single crystal data for $Lu_{14}Co_2In_3$. $Gd_{14}Co_3In_{2.7}$ [9] is related to the $Lu_{14}Co_2In_3$ type indides, however, the gadolinium compound shows an additional 4d Co2 site, defects on the 8g Co1 site, and a mixed Co/In occupancy on the 4c site. We have observed similar structural features for the family of new nickel compounds $RE_{14}Ni_3In_3$ ($RE = Sc, Y, Gd–Tm, Lu$) [10], which are formed only with the smaller rare earth elements. These indides also show an additional 4d Ni2 site, similar to $Gd_{14}Co_3In_{2.7}$, and some RE/In mixing of the 4c RE1 sites.

Since the structure refinement for $Lu_{14}Co_2In_3$ was carried out with 754 F values with $I > 6\sigma(I)$ and resulted in a somewhat high residual of $R = 0.061$ [6], we decided to reinvestigate these cobalt-based indides.

Table 1. Lattice parameters of tetragonal indides with $Lu_{14}Co_2In_3$ ($Gd_{14}Co_3In_{2.7}$) type structure, space group $P4_2/nmc$.

Compound	<i>a</i> (pm)	<i>c</i> (pm)	<i>V</i> (nm ³)	Reference
$Y_{14}Co_3In_3$	959.3(2)	2319.5(7)	2.1344	this work
$Y_{14}Co_2In_3$	953.0(3)	2326.9(8)	2.1400	[6]
$Gd_{14}Co_2In_3$	961.5(2)	2333.6(6)	2.1574	[6]
$Gd_{14}Co_3In_3$	961.7(2)	2330.3(8)	2.1552	[9]
$Tb_{14}Co_3In_3$	953.9(2)	2317.4(8)	2.1086	this work
$Tb_{14}Co_2In_3$	954.4(3)	2322.5(9)	2.1155	[6]
$Dy_{14}Co_3In_3$	950.0(2)	2296.9(6)	2.0728	this work
$Dy_{14}Co_2In_3$	950.0(3)	2300.2(9)	2.0759	[6]
$Ho_{14}Co_3In_3$	946.9(1)	2291.2(3)	2.0542	this work
$Ho_{14}Co_2In_3$	945.9(2)	2291.3(8)	2.0501	[6]
$Er_{14}Co_3In_3$	941.87(8)	2275.4(3)	2.0186	this work
$Er_{14}Co_2In_3$	941.3(3)	2279.3(9)	2.0196	[6]
$Tm_{14}Co_2In_3$	936.8(3)	2269.1(9)	1.9914	[6]
$Lu_{14}Co_2In_3$	933.3(2)	2263.3(4)	1.9714	[6]

The synthesis and structure refinements of $RE_{14}Co_3In_3$ ($RE = Y, Tb, Dy, Ho, Er$) are reported herein.

Experimental Section

Synthesis

Starting materials for the preparation of the $RE_{14}Co_3In_3$ samples were ingots of the rare earth metals (Johnson Matthey, Chempur or Kelpin), cobalt powder (Sigma-Aldrich, 100 mesh), and indium tear drops (Johnson-Matthey), all with stated purities better than 99.9%. All samples were prepared directly from the elements *via* arc-melting [11] under an atmosphere of *ca.* 600 mbar argon. The argon was purified before over titanium sponge (900 K), silica gel, and molecular sieves. The elements were weighed in the ideal 14 : 3 : 3 atomic ratios. The cobalt powder was cold-pressed to small pellets ($\varnothing 6$ mm) prior to arc-melting. After the first melting stage, all samples were turned over and remelted two times in the arc-melting crucible in order to achieve homogeneity. The weight losses were always smaller than 0.5 weight-%. The $RE_{14}Co_3In_3$ indides were obtained as silvery buttons with metallic luster which are stable in air over months.

After the arc-melting procedure the $RE_{14}Co_3In_3$ indides were obtained only as polycrystalline powders. Single crystals were grown using special heat treatment. First the buttons were crushed, powdered and cold-pressed into pellets. Next the samples were put in small tantalum containers that were sealed in evacuated silica tubes as an oxidation protection. The ampoules were first heated to 1380 K for the Dy, Ho, and Er compounds (to 1360 K for Tb and to 1390 K for Y) within 5 h and held at that temperature for 6 h. Subsequently the temperature was lowered at a rate of 5 K/h to 950 K for all compounds, then at a rate of 10 K/h to 700 K, and finally cooled to room temperature within 10 h. As a result in all cases single crystals of irregular shape were ob-

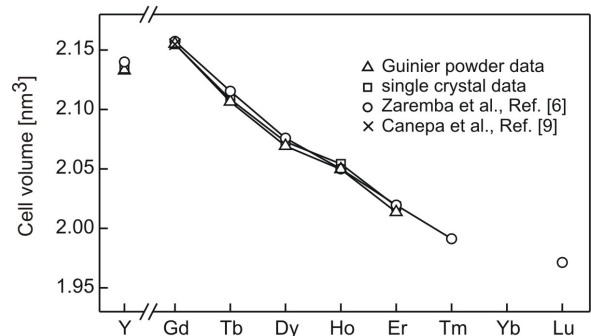


Fig. 1. Plot of the cell volumes of the tetragonal $RE_{14}Co_3In_3$ indides.

tained. After cooling, the samples could easily be separated from the tantalum container. No reaction of the samples with tantalum could be detected.

X-ray film data and structure refinements

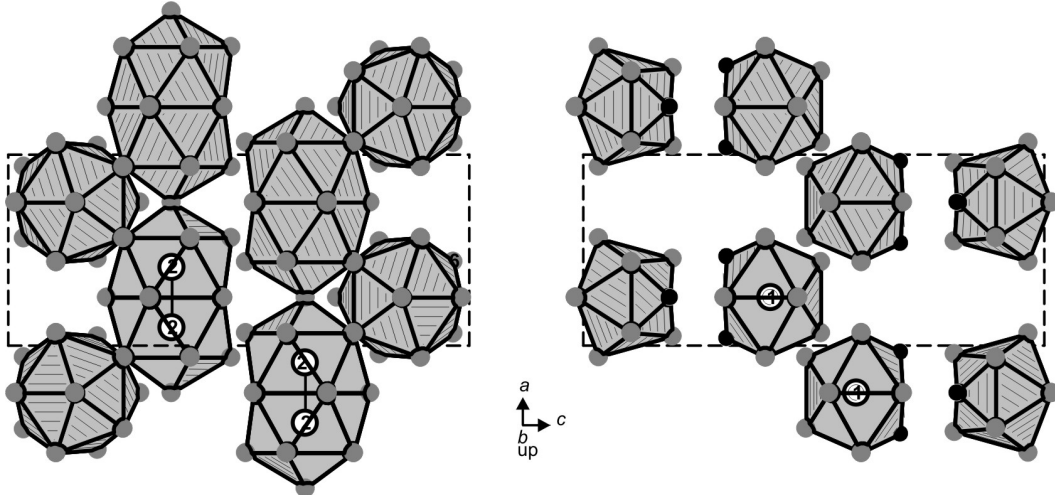
The arc-melted and the annealed samples were checked through Guinier powder patterns (α -quartz ($a = 491.30$, $c = 540.46$ pm) as an internal standard) using $Cu-K\alpha_1$ radiation. The Guinier camera was equipped with an imaging plate system (Fujifilm BAS-1800). The experimental patterns matched with calculated ones [12] using the atomic positions obtained from the structure refinements. The lattice parameters (Table 1 and Fig. 1) are in good agreement with the previously published data [6, 9]. The small discrepancies, especially for the *c* parameters, reflect the small homogeneity ranges.

Irregularly shaped single crystals of $RE_{14}Co_3In_3$ ($RE = Y, Tb, Dy, Ho, Er$) were isolated from the annealed samples by mechanical fragmentation and examined by Laue photographs on a Buerger precession camera (equipped with an imaging plate system Fujifilm BAS-1800) in order to establish suitability for intensity data collection. Intensity data were collected at room temperature by use of a Stoe IPDS-II diffractometer with graphite monochromatized $Mo-K\alpha$ radiation. The absorption corrections were numerical. All relevant crystallographic data for the data collections and evaluations are listed in Table 2.

Careful examination of the five data sets revealed space group $P4_2/nmc$ for the $RE_{14}Co_3In_3$ compounds, in agreement with all previous investigations [6, 9, 10]. The atomic parameters of $Gd_{14}Ni_{3.29}In_{2.71}$ [10] were taken as starting values and the structures were refined using SHELXL-97 (full-matrix least-squares on F_o^2) [13] with anisotropic atomic displacement parameters for all sites. Since the nickel compounds revealed RE/In and Ni/In mixing on the two $4c$ sites, the occupancy parameters were refined in separate series of least-squares cycles. All $RE_{14}Co_3In_3$ compounds revealed defects on the $8g$ Co1 site and In/Co mixing on

Table 2. Crystal data and structure refinement for $Y_{13.90(1)}Co_{2.99(1)}In_{3.02(1)}$, $Tb_{13.92(2)}Co_{3.01(2)}In_{2.92(2)}$, $Dy_{13.90(2)}Co_{2.97(2)}In_{2.95(2)}$, $Ho_{14}Co_{2.80(2)}In_{2.89(2)}$, and $Er_{13.83(2)}Co_{2.88(2)}In_{3.10(2)}$, space group $P4_2/nmc$, $Z = 4$.

Empirical formula	$Y_{13.90}Co_{2.99}In_{3.02}$	$Tb_{13.92}Co_{3.01}In_{2.92}$	$Dy_{13.90}Co_{2.97}In_{2.95}$	$Ho_{14}Co_{2.80}In_{2.89}$	$Er_{13.83}Co_{2.88}In_{3.10}$
Molar mass [g/mol]	1765.99	2746.13	2796.25	2830.27	2862.89
Unit cell dimensions (Single crystal):					
a [pm]	959.0(1)	953.8(1)	949.24(3)	946.3(1)	941.0(1)
c [pm]	2319.1(5)	2315.8(5)	2296.5(1)	2289.0(5)	2274.2(5)
V [nm ³]	2.1328	2.1066	2.0693	2.0497	2.0137
Calculated density [g/cm ³]	5.50	8.66	8.98	9.17	9.44
Crystal size [μm^3]	$30 \times 110 \times 150$	$40 \times 70 \times 150$	$60 \times 60 \times 110$	$30 \times 70 \times 110$	$40 \times 70 \times 140$
Transmission (max : min)	6.75	2.04	3.26	1.99	2.47
Absorption coefficient [mm ⁻¹]	43.0	51.7	55.4	58.9	63.3
Detector distance [mm]	70	60	60	60	60
Exposure time [min]	12	12	12	12	12
ω Range; increment [°]	0–180; 1.0	0–180; 1.0	0–180; 1.0	0–180; 1.0	0–180; 1.0
Integr. param. A, B, EMS	11.5; 3.5; 0.016	10.5; 1.0; 0.014	9.6; 2.2; 0.012	9.0; 4.0; 0.022	10.0; 1.0; 0.016
F(000)	3096	4552	4608	4664	4720
θ Range [°]	2 to 34	3 to 34	3 to 36	2 to 34	2 to 36
Range in hkl	$\pm 14, \pm 14, \pm 35$	$\pm 15, \pm 15, \pm 36$	$\pm 15, \pm 15, \pm 37$	$\pm 14, \pm 13, \pm 36$	$\pm 15, \pm 15, \pm 36$
Total no. reflections	27019	28267	30178	25304	29132
Independent reflections	2289	2357	2518	2297	2450
Reflections with $I > 2\sigma(I)$	($R_{int} = 0.058$)	($R_{int} = 0.061$)	($R_{int} = 0.083$)	($R_{int} = 0.099$)	($R_{int} = 0.076$)
	2076	2163	2262	2001	2168
Data / parameters	($R_{sigma} = 0.021$)	($R_{sigma} = 0.023$)	($R_{sigma} = 0.032$)	($R_{sigma} = 0.039$)	($R_{sigma} = 0.028$)
	2289 / 65	2357 / 65	2518 / 65	2297 / 64	2450 / 65
Goodness-of-fit on F^2	1.216	1.095	1.094	1.124	1.090
Final R indices [$I > 2\sigma(I)$]	$R1 = 0.036$	$R1 = 0.041$	$R1 = 0.050$	$R1 = 0.042$	$R1 = 0.054$
	$wR2 = 0.054$	$wR2 = 0.105$	$wR2 = 0.122$	$wR2 = 0.096$	$wR2 = 0.135$
R Indices (all data)	$R1 = 0.043$	$R1 = 0.045$	$R1 = 0.057$	$R1 = 0.051$	$R1 = 0.061$
	$wR2 = 0.055$	$wR2 = 0.108$	$wR2 = 0.129$	$wR2 = 0.099$	$wR2 = 0.140$
Extinction coefficient	0.00029(2)	0.00064(5)	0.00058(4)	0.00061(3)	0.0065(5)
Largest diff. peak and hole [e/Å ³]	1.56 and –1.63	5.01 and –3.64	4.79 and –4.26	3.59 and –3.13	4.55 and –4.26

Fig. 2. View of the $Ho_{14}Co_{2.80}In_{2.89}$ structure along the b axis. In the drawing on the left the condensation of the In_2 coordination polyhedra is presented. The In_1/Co_3 polyhedra are shown on the right. For details see text.

the $4c$ In_1 site. Except for the holmium compound we also observed RE/In mixing on the $4c$ RE_1 site, similar to the $RE_{14}Ni_3In_3$ indides [10]. Final difference Fourier synthe-

sis revealed no significant residual peaks (see Table 2). The highest residual densities were close to the rare earth positions and most likely resulted from incomplete absorption

Atom	Wyckoff site	Occupancy/%	x	y	z	U_{eq}
$Y_{13.90(1)}Co_{2.99(1)}In_{3.02(1)}$						
Y1/ In3	4c	90(1)/10(1)	3/4	1/4	0.14562(4)	133(3)
Y2	4d	100	1/4	1/4	0.21463(4)	112(2)
Y3	8g	100	1/4	0.54772(7)	0.30495(3)	131(1)
Y4	8g	100	1/4	0.56055(7)	0.98435(3)	126(1)
Y5	8f	100	0.56075(5)	—x	1/4	143(1)
Y6	8g	100	1/4	0.43837(6)	0.46725(3)	116(1)
Y7	16h	100	0.43540(5)	0.43377(5)	0.10499(2)	117(1)
Co1	8g	95.3(5)	1/4	0.53240(11)	0.18841(4)	161(3)
Co2	4d	100	1/4	1/4	0.55104(6)	153(2)
In1/ Co3	4c	91.9(9)/8.1(9)	3/4	1/4	0.90665(3)	117(2)
In2	8g	100	1/4	0.40987(5)	0.85479(2)	119(1)
$Tb_{13.92(2)}Co_{3.01(2)}In_{2.92(2)}$						
Tb1/ In3	4c	92(2)/8(2)	3/4	1/4	0.14562(4)	159(3)
Tb2	4d	100	1/4	1/4	0.21426(4)	146(2)
Tb3	8g	100	1/4	0.54739(7)	0.30493(3)	179(1)
Tb4	8g	100	1/4	0.56021(6)	0.98421(3)	167(1)
Tb5	8f	100	0.56132(5)	—x	1/4	172(1)
Tb6	8g	100	1/4	0.43956(6)	0.46686(3)	154(1)
Tb7	16h	100	0.43564(4)	0.43429(4)	0.10501(2)	147(1)
Co1	8g	93(1)	1/4	0.5335(2)	0.18804(9)	195(6)
Co2	4d	100	1/4	1/4	0.5500(1)	204(5)
In1/ Co3	4c	84(2)/16(2)	3/4	1/4	0.90641(6)	158(4)
In2	8g	100	1/4	0.40849(9)	0.85469(3)	146(2)
$Dy_{13.90(2)}Co_{2.97(2)}In_{2.95(2)}$						
Dy1/ In3	4c	90(2)/10(2)	3/4	1/4	0.14548(5)	159(3)
Dy2	4d	100	1/4	1/4	0.21423(5)	144(2)
Dy3	8g	100	1/4	0.54753(9)	0.30503(4)	179(2)
Dy4	8g	100	1/4	0.56038(8)	0.98442(4)	165(2)
Dy5	8f	100	0.56150(6)	—x	1/4	174(2)
Dy6	8g	100	1/4	0.43960(8)	0.46705(3)	153(2)
Dy7	16h	100	0.43599(6)	0.43392(6)	0.10500(2)	147(1)
Co1	8g	91(1)	1/4	0.5329(3)	0.1883(1)	184(7)
Co2	4d	100	1/4	1/4	0.5506(2)	200(6)
In1/ Co3	4c	86(2)/14(2)	3/4	1/4	0.90652(8)	160(5)
In2	8g	100	1/4	0.4089(1)	0.85470(5)	142(2)
$Ho_{14}Co_{2.80(2)}In_{2.89(2)}$						
Ho1	4c	100	3/4	1/4	0.14515(4)	131(2)
Ho2	4d	100	1/4	1/4	0.21353(4)	113(2)
Ho3	8g	100	1/4	0.54720(7)	0.30422(3)	139(1)
Ho4	8g	100	1/4	0.55986(6)	0.98435(3)	124(1)
Ho5	8f	100	0.56218(5)	—x	1/4	150(1)
Ho6	8g	100	1/4	0.43960(6)	0.46775(3)	117(1)
Ho7	16h	100	0.43607(5)	0.43421(5)	0.10499(2)	114(1)
Co1	8g	84(1)	1/4	0.5345(3)	0.1886(1)	165(7)
Co2	4d	100	1/4	1/4	0.5524(1)	163(5)
In1/ Co3	4c	89(2)/11(2)	3/4	1/4	0.90624(6)	121(4)
In2	8g	100	1/4	0.40870(10)	0.85458(4)	115(2)
$Er_{13.83(2)}Co_{2.88(2)}In_{3.10(2)}$						
Er1/ In3	4c	83(2)/17(2)	3/4	1/4	0.14542(5)	148(4)
Er2	4d	100	1/4	1/4	0.21399(5)	133(2)
Er3	8g	100	1/4	0.54687(9)	0.30470(4)	157(2)
Er4	8g	100	1/4	0.56014(9)	0.98440(4)	148(2)
Er5	8f	100	0.56196(7)	—x	1/4	163(2)
Er6	8g	100	1/4	0.43934(8)	0.46734(4)	138(2)
Er7	16h	100	0.43716(6)	0.43338(6)	0.10505(2)	135(1)
Co1	8g	91(2)	1/4	0.5328(3)	0.1878(1)	166(8)
Co2	4d	100	1/4	1/4	0.5520(2)	165(6)
In1/ Co3	4c	93(3)/7(3)	3/4	1/4	0.90661(8)	143(6)
In2	8g	100	1/4	0.4099(1)	0.85474(5)	137(2)

Table 3. Atomic coordinates and isotropic displacement parameters for

$Y_{13.90(1)}Co_{2.99(1)}In_{3.02(1)}$,
 $Tb_{13.92(2)}Co_{3.01(2)}In_{2.92(2)}$,
 $Dy_{13.90(2)}Co_{2.97(2)}In_{2.95(2)}$,
 $Ho_{14}Co_{2.80(2)}In_{2.89(2)}$, and
 $Er_{13.83(2)}Co_{2.88(2)}In_{3.10(2)}$.

U_{eq} (pm²) is defined as one third of the trace of the orthogonized U_{ij} tensor.

Table 4. Interatomic distances (pm) in the structure of $Ho_{14}Co_{2.80(2)}In_{2.89(2)}$. Standard deviations are equal or less than 0.3 pm. All distances within the first coordinate spheres are listed. The Co1 site is occupied only by 84(1)%.

Ho1: 2 In2	323.0	Ho5: 2 In2	331.6	Co1: 1 Ho3	264.9
2 Ho4	346.8	2 Ho3	336.7	1 Ho2	275.2
4 Ho5	347.5	2 Co1	339.7	2 Ho7	276.9
4 Ho7	356.5	2 Ho1	347.5	2 Ho3	280.5
Ho2: 2 Co1	275.2	2 Ho7	352.8	1 In1/Co3	297.9
2 Ho3	349.6	2 Ho2	354.7	2 Ho5	339.7
4 Ho7	350.9	2 Ho5	355.5	Co2: 2 Ho6	264.0
4 Ho5	354.7	Ho6: 1 Co2	264.0	4 Ho7	275.5
2 In2	356.1	1 In1/Co3	325.7	2 Ho4	332.0
1 Co2	368.9	2 Ho4	345.9	1 Ho2	368.9
Ho3: 1 Co1	264.9	2 In2	349.1	In1/Co3: 2 Co1	297.9
2 Co1	280.5	1 Ho6	358.8	2 Ho3	302.3
1 In1/Co3	302.3	2 Ho7	359.3	2 Ho4	308.4
2 Ho5	336.7	2 Ho4	361.5	2 Ho6	325.7
2 In2	339.0	2 Ho7	361.7	4 Ho7	347.8
1 Ho2	349.6	1 Ho3	387.9	In2: 1 In2	300.4
2 Ho7	364.3	Ho7: 1 Co2	275.5	1 Ho1	323.0
2 Ho3	367.8	1 Co1	276.9	1 Ho4	329.7
1 Ho3	383.8	1 In2	344.8	2 Ho5	331.6
1 Ho6	387.9	1 In1/Co3	347.8	2 Ho3	339.0
Ho4: 1 In1/Co3	308.4	1 Ho4	348.4	2 Ho7	344.8
1 In2	329.7	1 Ho7	348.6	2 Ho6	349.1
1 Co2	332.0	1 Ho2	350.9	1 Ho2	356.1
2 Ho6	345.9	1 Ho7	352.2		
1 Ho1	346.8	1 Ho5	352.8		
2 Ho7	348.4	1 Ho1	356.5		
1 Ho4	359.9	1 Ho6	359.3		
2 Ho7	360.7	1 Ho4	360.7		
2 Ho6	361.5	1 Ho6	361.8		
		1 Ho3	364.3		

corrections of these strongly absorbing intermetallics. The refined positional parameters and interatomic distances are listed in Tables 3 and 4. Further details on the structure refinements are available.*

EDX analyses

The bulk samples and the single crystals measured on the diffractometers have been analyzed by EDX using a LEICA 420 I scanning electron microscope with Y, TbF₃, DyF₃, HoF₃, ErF₃, Co, and InAs as standards. The single crystals mounted on the quartz fibres were coated with a thin carbon film. Pieces of the bulk samples were polished with different silica and diamond pastes and left unetched for the analyses in the scanning electron microscope in backscattering mode. The EDX analyses revealed no impurity elements and were in agreement with the refined compositions.

Discussion

The $RE_{14}Co_3In_3$ intermetallics with Y, Tb, Dy, Ho, and Er as the rare earth components have been reinves-

*Details may be obtained from: Fachinformationszentrum Karlsruhe, D-76344 Eggenstein-Leopoldshafen (Germany), by quoting the Registry No.'s. CSD-415963 (Y_{13.90}Co_{2.99}In_{3.02}), CSD-415964 (Tb_{13.92}Co_{3.01}In_{2.92}), CSD-415965 (Dy_{13.90}Co_{2.97}In_{2.95}), CSD-415966 (Ho₁₄Co_{2.80}In_{2.89}), and CSD-415967 (Er_{13.83}Co_{2.88}In_{3.10}).

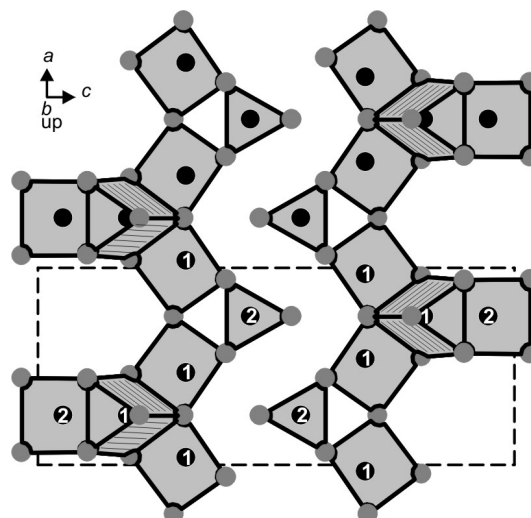


Fig. 3. Condensation of the trigonal prismatic units around the Co1 and Co2 atoms in the $Ho_{14}Co_{2.80}In_{2.89}$ structure (view along the b axis). For details see text.

tigated on the basis of X-ray single crystal data. These studies clearly revealed the additional cobalt position and the Co/In mixing on the $4c$ site, in agreement with a recent investigation on $Gd_{14}Co_{3.03}In_{2.69}$ [9]. Except for the holmium compound, a small degree of RE/In mixing was observed for the $4c$ $RE1$ position. These results nicely confirm those of our recent investigations on the series of $RE_{14}Ni_3In_3$ nickel indides [10].

The crystal chemistry of the cobalt compounds is more or less similar to that of the nickel compounds, with the exception that defects up to 16% have been observed for the Co1 sites, while all Ni1 sites in the $RE_{14}Ni_3In_3$ compounds were fully occupied. The origin of these defects is so far not understood. They are surprising, since the cobalt compounds already have the lower electron count.

Since the structure of the $RE_{14}Co_3In_3$ indides is relatively complex, the most descriptive presentation is the condensation of the coordination polyhedra. A large polyhedral building unit is formed around the In2 dumb-bells which have the short In2–In2 distance of 300 pm in $Ho_{14}Co_{2.80}In_{2.89}$ (Fig. 2, left-hand part). In view of the high rare earth metal content, this segregation is remarkable. The polyhedra around the In2 dumb-bells extend in the a or the b direction, a consequence of the 4_2 axis.

The arrangement of the polyhedra around the mixed occupied site In1/Co3 is presented in the right-hand part of Fig. 2. The twelve nearest neighbours are

arranged in the form of a significantly distorted icosahedron.

In $Ho_{14}Co_{2.80}In_{2.89}$ each cobalt atom has six nearest holmium neighbours in trigonal prismatic coordination (Fig. 3). These prisms are condensed *via* common edges and corners, leading to two-dimensional motifs. Due to the 4_2 axis, every other of these motifs is rotated by 90° . Interestingly, the defect Co1 site has a higher average Co1–Ho distance of 276 pm as compared to Co2–Ho of 272 pm.

The coordination polyhedra of all crystallographically independent sites and the interatomic distances have been discussed in detail for the series of $RE_{14}Ni_3In_3$ nickel indides [10]. For further information we refer to the previous work.

Acknowledgements

We thank H.-J. Göcke for the work at the scanning electron microscope. This work was supported by the Deutsche Forschungsgemeinschaft. V.I.Z. is indebted to the Alexander von Humboldt-Stiftung for a research grant.

-
- [1] Ya. M. Kalychak, J. Alloys Compd. **262–263**, 341 (1997).
 - [2] Ya. M. Kalychak, J. Alloys Compd. **291**, 80 (1999).
 - [3] Ya. M. Kalychak, V. I. Zaremba, R. Pöttgen, M. Lukachuk, R.-D. Hoffmann, Rare Earth-Transition Metal-Indides, in K. A. Gschneidner Jr., V. K. Pecharsky, J.-C. Bünzli, Handbook on the Physics and Chemistry of Rare Earths, Vol. 34, chapter 218, p. 1–133, Elsevier, Amsterdam (2005).
 - [4] Ya. M. Kalychak, V. I. Zaremba, J. Stępień-Damm, Ya. V. Galadzhun, L. G. Akselrud, Kristallografia (in Russian) **43**, 17 (1998).
 - [5] Ya. M. Kalychak, V. I. Zaremba, P. Yu. Zavalii, Z. Kristallogr. **208**, 380 (1993).
 - [6] V. I. Zaremba, Ya. M. Kalychak, P. Yu. Zavalii, Sov. Phys. Crystallogr. **37**, 178 (1992).
 - [7] M. Lukachuk, Ya. M. Kalychak, M. Dzevenko, R. Pöttgen, J. Solid State Chem. **178**, 1247 (2005).
 - [8] Ya. V. Galadzhun, V. I. Zaremba, Ya. M. Kalychak, V. M. Davydov, A. P. Pikul, J. Stępień-Damm, D. Kaczorowski, J. Solid State Chem. **177**, 17 (2004).
 - [9] F. Canepa, M. Napoletano, M. L. Fornasini, F. Merlo, J. Alloys Compd. **345**, 42 (2002).
 - [10] M. Lukachuk, Ya. V. Galadzhun, R. I. Zaremba, M. V. Dzevenko, Ya. M. Kalychak, V. I. Zaremba, U. Ch. Rodewald, R. Pöttgen, J. Solid State Chem. **178**, 2724 (2005).
 - [11] R. Pöttgen, Th. Gulden, A. Simon, GIT Labor Fachzeitschrift **43**, 133 (1999).
 - [12] K. Yvon, W. Jeitschko, E. Parthé, J. Appl. Crystallogr. **10**, 73 (1977).
 - [13] G. M. Sheldrick, SHELXL-97, Program for Crystal Structure Refinement, University of Göttingen, Germany (1997).